Comment: After the revision, most of my questions got feedback. The manuscript is well-organized and suitable for publication. Other simple questions which are just my curious points: Do the authors have any idea how many chlorophyll profiles from BGC-Argo are associated with SE and SSE eddies? Do SE and SSE exhibit any differences in the vertical chlorophyll distributions?

Response: To answer this question, we obtained the Biogeochemical Argo (BGC-Argo) floats from https://dataselection.euro-argo.eu/. BGC-Argo floats are equipped with conductivity-temperature-depth (CTD) sensors to measure physical variables and bio-optical sensors to measure biogeochemical variables. For each BGC-Argo profile, we selected the highest-level data mode (delayed mode), produced later (over 1 year), and required control and validation by a scientific expert. Only profile data flagged as good quality were considered in the study. In addition, we conducted quality control on chlorophyll-*a* (Chl-*a*) profiles. First, a three-point moving median filter was applied on each profile to remove spikes (Bisson et al., 2019; Haëntjens et al., 2020). Next, we followed the calibration procedure of Roesler et al. (2017) and Haëntjens et al. (2020) to adjust the Chl-*a* data using the following equation:

$$\text{Chl-}a' = (\text{Chl-}a - 0.019) / 2.32$$

Where Chl-*a*' represents the Chl-*a* profiles used in the study and Chl-*a* represents the BGC-Argo Chl-*a* profiles that remove spikes. After the above data preprocessing, we obtained 399 (491) BGC-Argo profiles within 1.5 radii of AEs (CEs) in the North Indian Ocean during 2000-2015. The spatial distribution of these BGC-Argo profiles is shown in Figure 1.

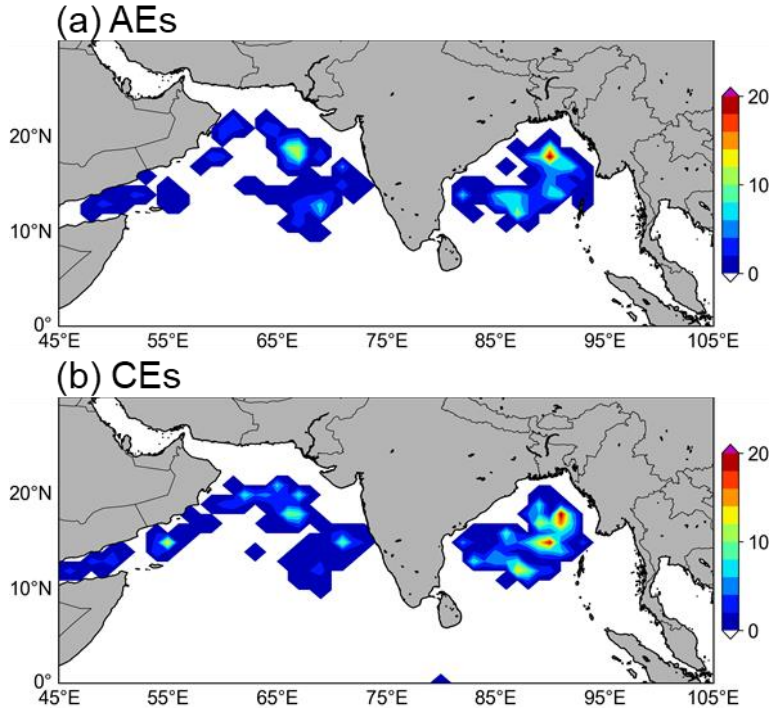

Figure 1. The distribution of numbers of BGC-Argo profiles occurred in the 1°×1° bins within 1.5 radii of AEs (a) and CEs (b) in the North Indian Ocean during 2000-2015.

However, one should note that not all the above BGC-Argo profiles can be used to analyze Chl-*a* within eddies. Quality control was applied to eddy-collocated BGC-Argo floats using the following criteria: (1) Chl-*a* data from the upper 10 m were excluded from analyses because large variability and high uncertainty were observed there (Su et al., 2021); (2) Besides, each profile must contain at least one data point at a depth of 200 m or greater. It is because the Chl-*a* is generally located at the base of the euphotic layer (50 - 200 m) in the North Indian Ocean (Mignot et al., 2014); (3) There are more than 5 observations between 10 m and 200 m. As a result, only 30 (45) BGC-Argo profiles within 1.5R of AEs (CEs) meet the above criteria. Among them, 18 (12) BGC-Argo profiles were found within 1.5R of SAEs (SSAEs), while 32 (13) BGC-Argo profiles were found within 1.5R of SCEs (SSCEs).

Despite the small number of BGC-Argo profiles, we can see the differences in Chl-*a* profiles between SAEs and SSAEs or SCEs and SSCEs. As shown in Figure 2a, Chl-*a* induced by SSAEs is significantly greater than that caused by SAEs in the upper 30 m. Besides, Chl-*a* induced by SSCEs is significantly less than that caused by SCEs in the upper 50 m (Figure 2b). Such a result is consistent with the distinct displacements of isopycnals within SSAEs and SSCEs shown in Figure 9 in the manuscript. The convex of isopycnals within SSAEs leads to the ascent of deeper water to the surface layer. This process facilitates the vertical transport of nutrients, promoting enhanced biological productivity and higher concentrations of Chl-*a* within SSAEs than SAEs. The vertical movement of water masses and the associated nutrient supply contribute to the favorable conditions for phytoplankton growth and the accumulation of Chl-*a* in SSAEs. Similarly, the concave of isopycnals within SSCEs leads to the subduction of surface water, resulting in lower Chl-*a* concentrations compared to SCEs.

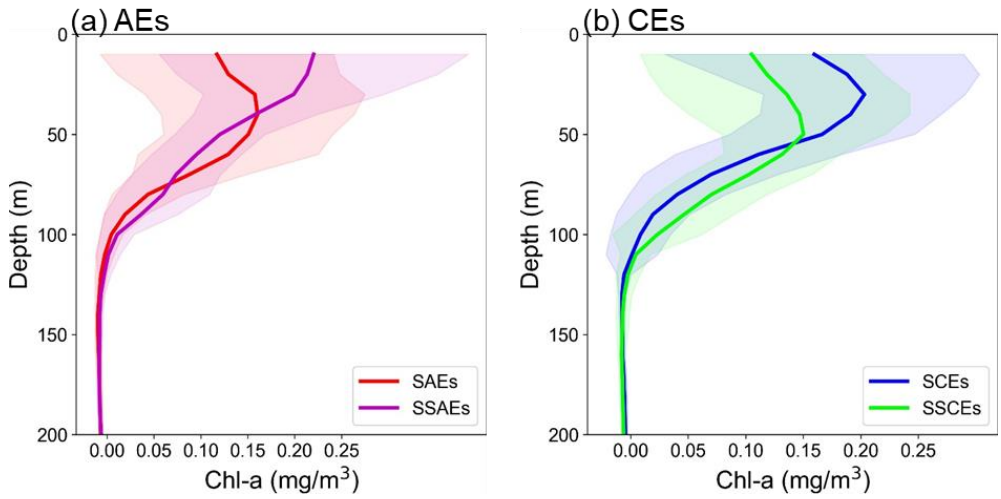

Figure 2. Mean (solid line) and standard deviation (shadow) values of Chl-*a* profiles for SAEs and SSAEs (a), and SCEs and SSCEs (b) in the North Indian Ocean.

According to the above results, we make the following modifications to the

manuscript: (1) add detailed information on BGC-Argo data, data preprocessing, and quality control in Section 2.1 Data; (2) add Figure 2 and its description and explanation in Section 4 Discussion; (3) add following references to the References part.

References

Bisson, K., Boss, E., Westberry, T., & Behrenfeld, M. (2019). Evaluating satellite estimates of particulate backscatter in the global open ocean using autonomous profiling floats. *Optics Express*, *27*(21), 30191-30203. https://doi.org/10.1364/OE.27.030191

Haëntjens, N., Della Penna, A., Briggs, N., Karp-Boss, L., Gaube, P., Claustre, H., & Boss, E. (2020). Detecting Mesopelagic Organisms Using Biogeochemical-Argo Floats. *Geophysical Research Letters*, *47*(6), e2019GL086088. https://doi.org/https://doi.org/10.1029/2019GL086088

Mignot, A., Claustre, H., Uitz, J., Poteau, A., d'Ortenzio, F., & Xing, X. (2014). Understanding the seasonal dynamics of phytoplankton biomass and the deep chlorophyll maximum in oligotrophic environments: A Bio-Argo float investigation. *Global Biogeochemical Cycles*, *28*(8), 856-876. https://doi.org/10.1002/2013GB004781

Roesler, C., Uitz, J., Claustre, H., Boss, E., Xing, X., Organelli, E., et al. (2017). Recommendations for obtaining unbiased chlorophyll estimates from in situ chlorophyll fluorometers: A global analysis of WET Labs ECO sensors. *Limnology and Oceanography: Methods*, *15*(6), 572-585. https://doi.org/https://doi.org/10.1002/lom3.10185

Su, J., Strutton, P. G., & Schallenberg, C. (2021). The subsurface biological structure of Southern Ocean eddies revealed by BGC-Argo floats. *Journal of marine systems*, *220*, 103569. https://doi.org/10.1016/j.jmarsys.2021.103569